

Reversible separation of single-walled carbon nanotubes in bundles

Sangeeta Sahoo,^{1,a)} Ravi Maranganti,² Sarah Lastella,¹ Govind Mallick,³ Shashi Karna,³ Pradeep Sharma,² and Pulickel M. Ajayan⁴

¹Department of Materials Science and Engineering, Rensselaer Polytechnic Institute, Troy, New York 12180-3590, USA

²Department of Mechanical Engineering, University of Houston, Houston, Texas 77204, USA

³AMSRD-ARL-WM-BD, Weapons & Materials Directorate, US Army Research Laboratory, Aberdeen Proving Ground, Maryland 21005-5069, USA

⁴Department of Mechanical Engineering and Materials Science, Rice University, 6100 Main Street, Houston, Texas 77005, USA

(Received 24 June 2008; accepted 8 August 2008; published online 29 August 2008)

We show that electrostatic charging of nanotubes and the consequent repulsion can lead to reversible separation of individual single-walled carbon nanotubes in bundles. Low-energy electron beam irradiation leads to this completely reversible phenomenon. A simple semianalytical model is used to explain the observed separation mechanism. The reversibility of the separation process is attributed to discharging and thermal-fluctuation induced motion of the nanotubes in ambient air. Further, the separation impacts the electrical conductance of small nanotube bundled devices. © 2008 American Institute of Physics. [DOI: 10.1063/1.2976631]

Due to their interesting electrical properties, single-walled carbon nanotubes (SWNTs) have been considered as promising candidates for nanoelectronic devices. However, due to strong van der Waals (vdW) interaction between SWNTs, they have a natural tendency to form bundles,¹ which makes the realization of single SWNT-based applications very challenging. Therefore, more investigations are needed toward the debundling mechanism of SWNTs.

Most of the existing debundling techniques follow various wet chemical routes. Here, we report a distinct approach to separate SWNTs in bundles using low-energy electron irradiation. Over the past decade, a number of studies^{2–6} have demonstrated the use of high energy e-beam and/or ion beam irradiation for annealing metallic contacts,^{6,7} coalescence of carbon nanotubes (CNTs), and exfoliation of CNT bundles.⁸ In the present work, we show that SWNTs in a rope can be separated under e-beam irradiation in scanning electron microscope (SEM) at a relatively low voltage range. The separation process occurs along any desired part of the rope locally exposed to the electron irradiation. Theoretical studies suggest an active role of electrostatic charging of nanotubes to the separation process. In addition, the electrical measurements of individual small nanotube bundled devices show a reduction in the conductance due to the separation. Furthermore, at room temperature, in the presence of ambient air, the separated nanotubes are observed to return to their original packed state indicating a reversible separation process due to electron irradiation.

We have grown SWNTs on Si substrates covered with a 100 nm thick oxide layer using the chemical vapor deposition method.⁹ SWNT bundles were then exposed to e-beam irradiation in an SEM (Supra-55) at voltage ranges of 1–5 keV and with a current density in the range of 0.8–20 mA/cm². Two-terminal electrical devices based on individual SWNT ropes were fabricated using conventional e-beam lithography followed by e-beam evaporation of a 50 nm thick Au layer on top of a thin (≈ 5 –10 nm) Ti layer.

Finally, the current-voltage (I - V) measurements were conducted at room temperature on a microtip probe station equipped with a Keithley 4200 source measure unit.

Figures 1(a), 1(c), and 1(e) exhibit the SEM images of three different SWNT bundles before exposure to an extensive irradiation in SEM. These three bundles have been exposed to electron irradiation in SEM at 2.5 keV for 15–20 s. After irradiation, the same bundles are shown in Figs. 1(b), 1(d), and 1(f), respectively. The separation for each of these bundles into two thinner parts (smaller bundles/individual SWNTs) is very clear from these images. We have imaged a pristine [Fig. 1(g)] and two other separated SWNT bundles [Figs. 1(h) and 1(i)] in a tapping mode atomic force microscope (AFM). The appearance of two distinct clear separated nanotubes (single SWNT or thinner bundle) in Figs. 1(h) and 1(i) evidently ensures the separation of the bundle under electron irradiation. Note that the number of SWNTs in each of these bundles is not same. However, only two thinner separated parts have been resolved successfully within the scope of this study.

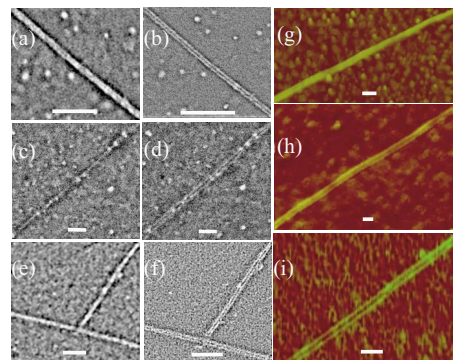


FIG. 1. (Color online) SEM micrographs of three SWNT bundles before [(a), (c), and (e)] and after [(b), (d), and (f)] separation, respectively. Tapping mode AFM images of a pristine bundle (g) before exposure and two separated bundles (h), (i) after exposure to electron irradiation, respectively. The scale bar is 100 nm.

^{a)}Electronic mail: sahoos@rpi.edu.

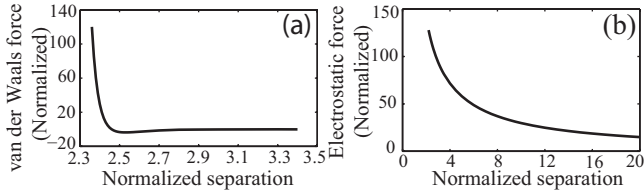


FIG. 2. Comparison between the vdW interaction force and the electrostatic interaction force between two parallel (10,10) CNTs with respect to the perpendicular distance between them. The distance is normalized by the radius of the (10,10) nanotube and the forces are normalized with respect to a force amount to the vdW well depth at equilibrium per unit radius.

It has been observed that nanotubes are prone to charging upon e-beam irradiation, especially while being supported on insulating substrates.^{10–12} To investigate the effects of electrostatic charging on separation, we have carried out a simple semianalytical calculation. Initially, before e-beam irradiation, we assume that the SWNTs interact solely through vdW forces leading to the existence of an equilibrium separation between two SWNTs. Based on the continuum Lennard–Jones model, the vdW interaction potential between two parallel CNTs, spaced apart by a perpendicular distance of ρ and with radii of R_i and R_j , respectively, is given by¹³

$$\phi_{ij} = \int_0^{2\pi} \theta R_j V(\sqrt{R_j^2 + \rho^2 - 2\rho R_j \cos(\alpha)}, R_i) d\alpha. \quad (1)$$

The potential V is defined as

$$V(r, R) = 3\pi\theta^2\epsilon\sigma^2 \left[\frac{21}{31} \left(\frac{\sigma}{R}\right)^{10} \left(\frac{R}{r}\right)^{11} M_{11}\left(\frac{R}{r}\right) - \left(\frac{\sigma}{R}\right)^4 \left(\frac{R}{r}\right)^5 M_5\left(\frac{R}{r}\right) \right]. \quad (2)$$

Furthermore, M_{11} and M_5 are the elliptic integrals which must be evaluated numerically as $M_n(z) = \int_0^\pi d\beta (1+z^2 - 2z \cos\beta)^{-n/2}$. In Eq. (1), θ is the surface density of carbon atoms (≈ 0.37 atoms/ \AA^2 for a graphene sheet). In Eq. (2), ϵ and σ are the usual vdW parameters. The vdW interaction force, shown in Fig. 2(a), is given by the derivative of the interaction energy with respect to the separation distance between two parallel (10,10) CNTs. The equilibrium separation distance between the two nanotubes is 2.46 times the radius of the (10,10) nanotube (≈ 0.673 nm) [Fig. 2(a)].

During electron irradiation, the amount of charge retained by the nanotube depends upon several factors such as the magnitude of the beam current, the conductivity of the substrate, and the amount of secondary emission, among others. However, we emphasize here that beyond an initial amount deposited on the CNT, subsequent incident electrons are repulsed by the existing layer. Hence, prolonged additional exposure should have no effect on the separation distance. Therefore, if we assume that the charge resides on the surface of the metallic (10,10) nanotubes, the present picture deals with two charged conducting hollow cylinders interacting via electrostatic forces. The radially symmetric electric field due to an infinitely long charged cylinder of radius a at a distance r from its center can be calculated by Gauss's law, $E(r) = qa/\epsilon_0 r$, where q is the surface charge density while ϵ_0 is the permittivity of free space. The force exerted by the field on a unit length of the second nanotube lying at a distance d can be derived as

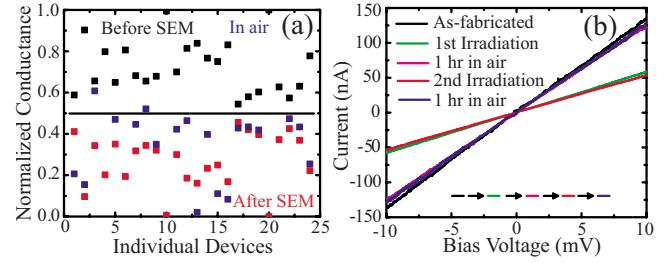


FIG. 3. (Color online) (a) Collection of normalized conductance of individual devices. The black, blue, and red points present the conductance values before separation, after separation, and in ambient air for few hours after separation, respectively. Conductance is normalized by the sum of the conductance values before (G_b) and after (G_a) separation. (b) A collection of I - V for a device at each step during an alternative exposure to e-beam irradiation and ambient air. The sequences are indicated by the arrows.

$$\frac{2q^2a^2}{\epsilon_0} \int_0^\pi \left\{ \frac{1}{\sqrt{d^2 + a^2 - 2ad \cos(\theta)}} \times \cos \left[\tan^{-1} \left(\frac{a \sin(\theta)}{d - a \cos(\theta)} \right) \right] \right\} d\theta. \quad (3)$$

Using the linear charge density of $0.1 e/\text{\AA}$,^{10,11} the surface charge density for the (10,10) nanotube can be estimated as $0.1e/(2\pi a) \approx 3.78 \times 10^{-21}$ C/ \AA .^{8,11} The electrostatic force is displayed in Fig. 2(b). It should be noted that in the vicinity of the vdW equilibrium separation of 2.46 units, the electrostatic force is at least an order of magnitude higher than the vdW force and hence will result in the separation of the nanotubes. Also, the electrostatic force falls off much slower than the vdW force. Thus, charging and hence the ensuing Coulombic repulsion is likely to be the dominant mechanism for the irradiation-induced separation in SEM.

The I - V measurements have been carried out on a total of 24 devices before and after exposure to electron irradiation at room temperature. The conductance for each device is extracted from the linear I - V characteristics and normalized with respect to the sum of the conductance values before (G_b) and after (G_a) separation. The normalized conductance for each device before (after) separation, $G_{b(a)}/(G_b + G_a)$, is presented by black (red) points in Fig. 3(a). The solid black line at the middle corresponds to the instance where conductance remains unaffected by the separation, i.e., $G_a = G_b$. In Fig. 3(a), none of the devices possesses conductance values on the middle line, ensuring a strong electrical dependence on the physical separation. Besides, for all the devices, conductance after separation (red points) takes place below the black line, whereas the conductance before separation (black points) stays above, indicating a reduction in conductance for each device that has undergone a separation process in SEM.

To investigate the stability of the separation between the nanotubes in ambient air, 19 out of the 24 devices were exposed to air at room temperature for one to a few hours. Corresponding conductance values are presented by the blue scattering points in Fig. 3(a). The majority (14) of the devices begin to approach their as-fabricated conductance values in the presence of ambient air. Now, if the increased conductance indicates a slow recombining process of the separated nanotubes in the presence of air, then the conductance should eventually attain the as-fabricated value for the reversible case. In Fig. 3(b), for a device with alternating exposure to e-beam irradiation and to ambient air, we have

shown the reversible nature of the separation process by measuring I - V at each step. Initially, after the first irradiation, the device was exposed to air for 1 h. As expected, the first SEM exposure reduces the current from the black to the green curve in Fig. 3(b). After 1 h exposure in air, the current (the magenta curve) reaches at almost the as-fabricated value (the black curve). At this stage, the device was exposed to the irradiation for second time. This time, after attaining a critical distance between the separated nanotubes, no further separation was observed in SEM even for a longer duration of e-beam exposure. Again for the second time, current drops from the magenta to the red curve in Fig. 3(b). 1 h exposure to the air brings the current (the blue curve) back to its original one (the magenta). Thus, the reversible I - V characteristics indicate a reversible separation process between SWNTs in the presence of air (Supplementary material,¹⁴ Fig. 1 represents the reversible SEM images for this device). Furthermore, the conductance drop [from the black to the green curve in Fig. 3(b)] after the first irradiation is very close to that (from the magenta to the red curve) of the second irradiation. These results indicate the existence of a critical separation distance between the nanotubes and up to which nanotubes can be separated under e-beam irradiation.

With exposure to ambient air, the exfoliated nanotubes are likely to discharge through the air molecules. After discharging, the separation distance between the nanotubes is expected to fluctuate due to the thermal noise. By considering the nanotube as a vibrating rod pinned at both ends, the thermal vibration amplitude δ of a nanotube is given as¹⁵ $\delta = [4L^3KT/\pi^4YdG(d^2+G^2)]^{1/2}$, where, d is the diameter, L is the length in nm, Y is Young's modulus of the nanotube, and G is the vdW distance in graphite. The thermal vibration amplitude δ , for a 1000 nm long (10,10) nanotube with Young's modulus of 1 TPa at 300 K is around 4.2 nm, which is about 6.24 normalized distance units. If we assume that the nanotubes are at a distance of 10 units from each other due to electrostatic repulsion, upon removal of the electron beam (and after discharging), thermal vibrations can bring the nanotubes as close as 3.76 units. This will then bring the

nanotubes back to a configuration where attractive vdW force will begin to operate.

In summary, we have demonstrated a charge induced separation process between SWNTs in SEM. Using a semi-analytical calculation, we have shown that the electrostatic charging effect is the likely mechanism for the splitting of nanotubes under e-beam exposure. In addition, the separation process has been shown to influence the electrical transport properties of SWNTs significantly. In the presence of air, a rebundling process between the separated nanotubes is reflected in the reversible I - V characteristics.

We acknowledge financial supports from RPI, IFC New York at RPI, Army Research Laboratory, and the National Science Foundation NSEC. S.S. thanks David Frey, Subbalakshmi Sreekala, and Sudhir Husale for their invaluable suggestions.

¹S. Nuriel, L. Liu, A. H. Barber, and H. D. Wagner, *Chem. Phys. Lett.* **404**, 263 (2005).

²A. V. Krasheninnikov, F. Banhart, J. X. Li, A. S. Foster, and R. M. Nieminen, *Phys. Rev. B* **72**, 125428 (2005).

³L. Sun, F. Banhart, A. V. Krasheninnikov, J. A. Rodriguez-Manzo, M. Terrones, and P. M. Ajayan, *Science* **312**, 1199 (2006).

⁴A. Kis, G. Csányi, J.-P. Salvetat, T.-N. Lee, E. Couteau, A. J. Kulik, W. Benoit, J. Brugger, and L. Forró, *Nat. Mater.* **3**, 153 (2004).

⁵Y. J. Jung, Y. Homma, R. Vajtai, Y. Kobayashi, T. Ogino, and P. M. Ajayan, *Nano Lett.* **4**, 1109 (2004).

⁶S. Gupta, R. J. Patel, N. Smith, R. E. Giedd, and D. Hui, *Diamond Relat. Mater.* **16**, 236 (2007).

⁷A. Bachtold, M. Henny, C. Terrier, C. Strunk, C. Schönberger, J.-P. Salvetat, J.-M. Bonard, and L. Forró, *Appl. Phys. Lett.* **73**, 274 (1998).

⁸L. Guan, Z. Shi, and Z. Gu, *Carbon* **43**, 1100 (2005).

⁹S. Lastella, H. Yang, D. Rider, I. Manners, P. M. Ajayan, and C. Y. Ryu, *J. Polym. Sci., Part B: Polym. Phys.* **45**, 758 (2007).

¹⁰M. Paillet, P. Poncharal, and A. Zahab, *Phys. Rev. Lett.* **94**, 186801 (2005).

¹¹P. Keblinski, S. K. Nayak, P. Zapol, and P. M. Ajayan, *Phys. Rev. Lett.* **89**, 255503 (2002).

¹²C. Li and T.-W. Chou, *Appl. Phys. Lett.* **89**, 063103 (2006).

¹³C.-H. Sun, G.-Q. Lu, and H.-M. Cheng, *Phys. Rev. B* **73**, 195414 (2006).

¹⁴See EPAPS Document No. E-APPLAB-93-013835. For more information on EPAPS, see <http://www.aip.org/pubservs/epaps.html>

¹⁵A. Krishnan, E. Dujardin, T. W. Ebbesen, P. N. Yianilos, and M. M. J. Treacy, *Phys. Rev. B* **58**, 14013 (1998).